

Reaction between barium and N₂O on large van der Waals clusters: progressive embedding of the BaO product inside argon and neon clusters

M. A. Gaveau,* M. Briant, P. R. Fournier, J. M. Mestdagh and J. P. Visticot

CEA/DSM/DRECAM/SPAM, CE Saclay, 91191, Gif-sur-Yvette Cedex, France.

E-mail: mgaveau@cea.fr

Received 9th November 1999, Accepted 17th December 1999

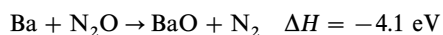
When a chemical reaction occurs at the surface of a cluster, the product can either be ejected or remain solvated within the cluster. This paper deals with the dynamics of the solvated product on various van der Waals clusters. This investigation is conducted on the Ba + N₂O reactive system by probing the chemiluminescence of the BaO product, either immediately after the reaction, or a few tens of microseconds later. It is shown that the interaction between BaO and the solvent increases along the sequence neon, argon, methane and nitrogen. The effect of varying the interaction time between the cluster and the solvated product is all the more pronounced when the solvent-product interaction is weak. It is very likely related to progressive embedding of the product inside the cluster.

1 Introduction

Numerous chemical processes do not occur in a single phase but proceed at the interface between different phases and are parts of the heterogeneous chemistry field. In order to investigate such chemical reactions at a microscopic level and to gain a better insight into their dynamics, it is important to study elementary processes, as it is done in the field of gas phase reactions where Roger Grice was so much active, by working under the single collision regime.¹ An ideal experiment would consist in isolating a single couple of reactants within a controlled reaction medium. For this purpose, we have developed in our laboratory a technique called CICR (cluster isolated chemical reactions), in which large van der Waals clusters model the solvent and are used as finite size chemical nanoreactors.^{2–4}

The CICR technique takes advantage of a gas phase formation of the van der Waals clusters, which makes this finite size reaction medium free from any perturbation due to a substrate. Due to their formation in a supersonic expansion, van der Waals clusters have a well defined internal energy and their size is ranging between 10² and 10⁴ atoms or molecules under our experimental conditions. Reactants are deposited on the clusters by collisional capture of the constituents of a low pressure buffer gas.⁵ This pick-up technique allows a strict control of the average number of reactants deposited per cluster.

The reactive Ba + N₂O system has been investigated in our laboratory on large van der Waals clusters, essentially because the reaction



has been extensively studied in the gas phase⁶ and produces chemiluminescent BaO molecules in the electronic states A¹Σ, A'¹Π and a³Σ. The Ba + N₂O system turned out to be a valuable example of chemical reaction at cluster surfaces. The first experiments performed by our group on argon clusters, proved that the reaction path is not dramatically affected by the cluster. The reaction still involves a single N₂O molecule and a single barium atom to produce the BaO molecule. Nevertheless, the cluster leads to specific effects on the product. In particular, the BaO molecule can be either ejected

from the cluster surface or stay solvated within the aggregate.⁷ The dynamics of the ejected product in CICR was not investigated on this particular system, but on the reaction Ba₃ + SF₆ → 2BaF + Ba + SF₄ ΔH = -4.9 eV performed on argon clusters,⁸ essentially for spectroscopic reasons.

The dynamics of solvation of the product after reaction at the cluster surface has not been investigated yet. The present paper aims to bring information concerning this process. We conduct this investigation on the Ba + N₂O system by probing the chemiluminescence of the BaO product, either immediately after the reaction, or a few tens of microseconds later. In the first case, the molecular reactant is deposited on clusters in the observation region (late pick-up configuration), so that the nascent chemiluminescent product is observed. In the second case, the N₂O pick-up is performed before the barium deposition (early pick-up configuration): in such conditions, the chemiluminescent product is detected a few tens of microseconds after the reaction occurrence. This is possible because BaO has a long lived a³Σ electronic state that lies 210 cm⁻¹ below the A¹Σ state the lifetime of which is 350 ns.⁹

The Ba + N₂O system was experimented on various van der Waals clusters, allowing to examine different interaction forces with the BaO product, ranging from weak with neon clusters to very strong with nitrogen ones. Reactive experiments on neon clusters are conducted for this purpose in the present work, both in the late and early pick-up configurations. Their results are compared with previous observations obtained on argon,⁷ methane¹⁰ and nitrogen clusters,² as well as with new observations concerning the BaO chemiluminescence from argon clusters under the early pick-up configuration.

2 Experiment

The experimental set-up is shown in Fig. 1. It features a supersonic free jet source (1 and 2 in the figure), a main chamber (3) which houses the optical diagnostics, and chambers (4 and 5) where mass spectrometers are used to characterize the cluster beam.

Van der Waals clusters are formed in a continuous supersonic free expansion from a Campargue molecular beam

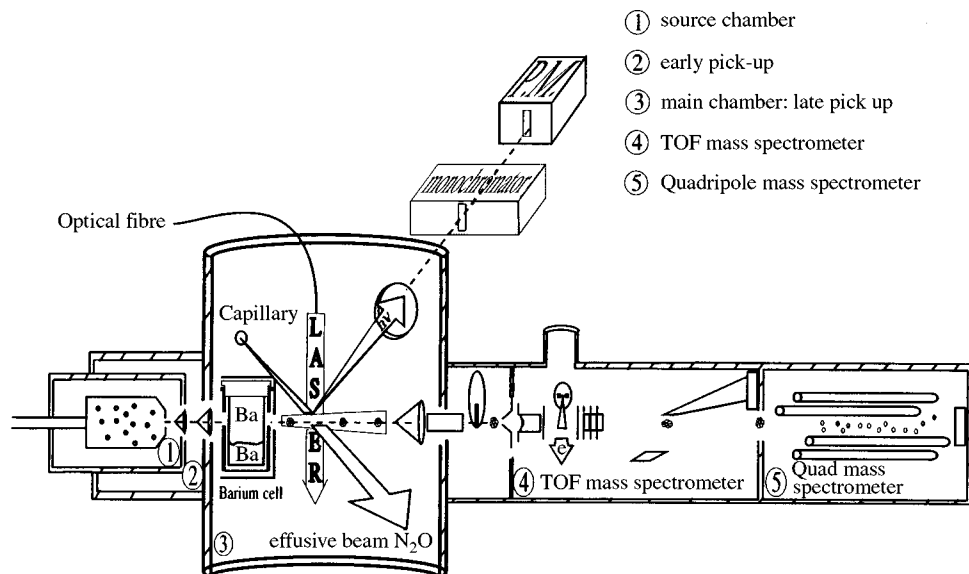


Fig. 1 Experimental set-up.

source.¹¹ The beam source conditions used in the present work depend mainly on the nature of the gas and on the desired cluster average size. The corresponding stagnation pressure P_0 and temperature T_0 as well as the nozzle type (sonic or conical) and diameter are listed in Table 1 for the various gases we used in the experiment, *i.e.* nitrogen, methane, argon and neon. The resulting mean cluster sizes are also listed in the table, together with the cluster temperatures when known from the theoretical and experimental works by Klots¹² and by Torchet *et al.*^{13,14}

The cluster beam is extracted from the free jet by a 1 mm skimmer and flies through a differentially pumped chamber, which can also be used as a pick-up chamber for the N_2O reactant. It is the early pick-up region.

The cluster beam is collimated prior to enter into the main chamber. There, it undergoes the pick-up of barium atoms inside a 30 mm long heated cell where a low pressure of barium vapor is maintained. Barium atoms are captured by the clusters during their course through the cell. Varying the temperature of the cell allows varying the barium vapor pressure and consequently the average number of barium atoms deposited on the clusters.

A second N_2O pick-up may be performed by crossing the cluster beam with a small effusive beam generated from a thin capillary tube, in a region (called hereafter the late pick-up region) located 17 mm downstream from the exit of the barium cell.

The late pick-up region is also the observation zone, from which fluorescence light is collected and focused onto the

entrance slit of a scanning grating monochromator. The luminescence signal is detected by a cooled photomultiplier tube (RCA 31034) working under the photon counting regime. After fast amplification and discrimination, the signal is accumulated using multiscaler cards implemented in a micro-computer. The spectra can be corrected for the spectral response of collection and detection on the whole wavelength range (410–900 nm) covered by the optical system. The total fluorescence signal is monitored by means of a second photomultiplier which collects a part of the undispersed light.

Fluorescence spectra have to be corrected in order to keep the relevant signal arising exclusively from cluster reactions. The cluster beam is flagged alternatively on and off in front of the pick-up zones and the two resulting spectra are subtracted in order to correct the signal for the undesirable background signal. It corresponds to two contributions measured with the cluster beam off, *i.e.* the blackbody radiation of the barium cell and the chemiluminescence signal of possible gas phase reactions between barium atoms effusing from the cell and the molecular reactant.

The chambers located downstream from the main chambers house a time-of-flight mass spectrometer and a quadrupole mass spectrometer. The former allows a direct measurement of the cluster size distribution. It is a log normal distribution, the width of which is equal to the average distribution size. This measurement can be biased by several phenomena such as fragmentation and multiple ionization processes or the lack of sensitivity of the detector for the very large masses. However, this determination can be double-checked by non-destructive

Table 1 Beam source conditions and resulting average cluster sizes and temperatures for the various experiments

gas	P_0 / K	T_0 / Type	Nozzle		Average cluster K	Cluster temperature/ K
			mm	Diameter/ size		
Nitrogen	28	293	Conical	0.08	3000	31 ± 4
Methane	13	226	Sonic	0.2	1200	~ 43
Argon	20	293	Sonic	0.2	2000	37 ± 5
Neon	30	80	Sonic	0.1	7000	10 ± 4

methods like the slow down technique¹⁵ and Rayleigh scattering¹⁶ with absolute and relative accuracies of 50 and 10%, respectively. The quadrupole mass spectrometer allows the determination of the relative fluxes of the volatile cluster constituents, by scattering the beam in the quadrupole chamber and measuring the resulting increases of partial pressures after a careful calibration of the quadrupole mass spectrometer.⁷

The cluster speed distribution can be obtained by measuring their time of flight along the beam, between a mechanical chopper and the quadrupole mass spectrometer.¹⁵ The flight path is 2275 mm long. Argon clusters generated at room temperature have an average speed of 500 m s⁻¹, whereas neon clusters formed from a source at much lower temperature (80 K) have an average speed of about 370 m s⁻¹.

We performed the reaction between Ba and N₂O on nitrogen, methane, argon and neon clusters in two different ways depending on which pick-up region was used. In the first one, the late pick-up region is used and N₂O is deposited onto clusters already carrying barium atoms. Thus the reaction occurs in this zone which is also the observation region from which fluorescence signals are detected. Such experiments document the nascent distribution of electronically excited BaO products during a few microseconds after the reaction, corresponding to the residence time of the clusters in the observation region. In the second type of experiment, N₂O is deposited on the clusters in the early pick-up region, before the pick-up of barium atoms. The reaction thus occurs in average in the middle of the barium cell: fluorescence signals are due to excited products several tens of microseconds after the reaction.

3 Experimental results

We first report the BaO chemiluminescence spectra recorded in neon cluster experiments for both late and early N₂O pick-up. They are plotted on panels d and g of Fig. 2 respectively, and their intensities are adjusted by an arbitrary factor for the

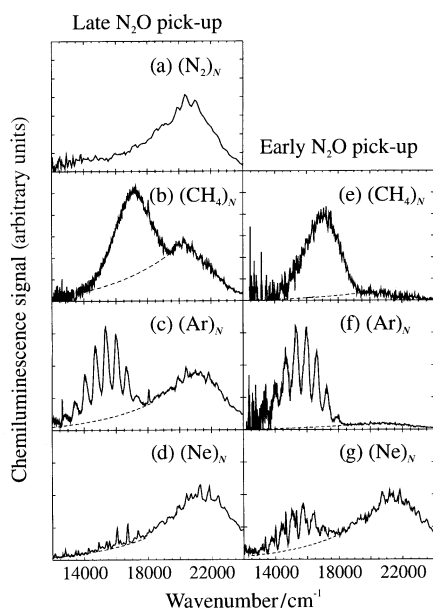


Fig. 2 Chemiluminescence spectra of the Ba + N₂O reaction on various van der Waals clusters. The left column corresponds to the late N₂O pick-up and the right column to the early N₂O pick-up. From top to bottom are successively presented spectra on nitrogen, methane, argon and neon clusters. The dashed line indicates the presumed contribution of the unstructured spectral component assigned to free BaO molecules ejected from clusters.

sake of visibility. These spectra are strikingly different from each other, particularly by their structured parts. The late pick-up chemiluminescence spectrum exhibits a very intense unstructured component covering the whole visible range. Over this quasi-continuous emission are superimposed several small narrow bands, that are regularly spaced between 11 500 and 18 000 cm⁻¹.

In the early pick-up experiment, the chemiluminescence yield is much weaker. The structured spectral component is enhanced with respect to the broad unstructured contribution. Ranging between 12 000 and 18 500 cm⁻¹, it exhibits two vibrational progressions with very different bandwidths.

The large difference between the chemiluminescence spectra recorded on neon clusters with the two different pick-up configurations led us to complement our set of experiments on argon by early pick-up experiments not available in our former publications. The resulting spectrum is plotted in Fig. 2 (panel f). It exhibits a vibrational progression that is composed of broad symmetric bands in the range 12 500–18 500 cm⁻¹. This intense structured contribution is superimposed to a very weak quasi-continuum covering the whole visible range. At least for the structured contributions, early and late pick-up spectra resemble more each other on argon clusters than on neon clusters. However, there are some differences that will be discussed in the next section. The methane and nitrogen results shown in Fig. 2 are taken from ref. 10 and 2, respectively. No spectrum is shown for the early pick-up configuration on N₂ clusters because no observable signal was obtained in this case.

4 Discussion

4.1 Reaction between Ba and N₂O on van der Waals clusters with a late N₂O pick-up

In this section, N₂O is deposited on clusters in the late pick-up region and the chemiluminescence spectra correspond to the emission of the nascent electronically excited product just after the chemical reaction. The left column of Fig. 2 compares the chemiluminescence spectra obtained with the late N₂O pick-up on nitrogen (panel a),² methane (panel b),¹⁰ argon (panel c)⁷ and neon (panel d) clusters.

The BaO chemiluminescence originating from the Ba + N₂O reaction on argon clusters (Fig. 2 panel c) has already been discussed in our former publications:⁷ it is a striking example of what can be the effect of the cluster on the chemical reaction occurring on its surface. We first recall this interpretation to enlighten the discussion for the neon clusters results. The chemiluminescence spectrum is formed of two broad components which are both assigned to BaO emission. The first one is a broad unstructured band that covers the whole visible range with a maximum around 21 000 cm⁻¹: it is very similar to the spectrum of the hot gas phase reaction product.⁶ The second component presents a pronounced vibrational structure and extends from 12 000 to 18 000 cm⁻¹. The spectrum also exhibits two barium atomic lines, the Ba(¹P₁ → ¹S₀) and Ba(³P₁ → ¹S₀) lines, respectively at 18 060.3 and 12 636.6 cm⁻¹, resulting from the presence of a small fraction of clusters in the beam carrying several Ba atoms. We have shown that the unstructured spectral feature can be assigned to the emission of hot free BaO molecules which have been ejected from the cluster just after their formation at the surface of the cluster.⁷ The structured feature is due to BaO molecules that stay solvated on the clusters. They are vibrationally relaxed by the cold argon medium. This vibrational progression has a strong similarity with the BaO spectrum in argon matrix¹⁷ and is therefore assigned to the BaO transitions A ¹Σ, a ³Σ (v' = 0) → X ¹Σ (v'').⁷ The interaction of

the solvated BaO molecules with the cluster environment induces a broadening and a 750 cm^{-1} blue shift of these bands with respect to the corresponding transitions of the free molecule.¹⁸ These solvated BaO bands are analysed in more detail in section 4.3 after subtraction of the underlying emission of free BaO.

All the chemiluminescence spectra obtained with the late N_2O pick-up whatever the nature of the cluster (Fig. 2 left column) present the same broad unstructured spectral component, that covers the whole visible range and is assigned to the free BaO molecules ejected from the cluster just after the reaction. Concerning this emission the main difference is a slight increasing red shift of its maximum from neon to argon, methane and nitrogen.

In contrast, the emission assigned to solvated BaO changes dramatically with the nature of the cluster. On methane clusters (panel b), the band structure of the solvated BaO component is completely washed out. It is replaced by a broad unstructured emission that has exactly the same shape as the envelope of the solvated BaO component from an argon cluster.¹⁰ Nevertheless, it is much more shifted to the blue of this latter spectrum. On nitrogen clusters (panel a), emission from solvated BaO has completely disappeared. This evolution reflects an increasing interaction between BaO and the cluster from argon to nitrogen. Interaction between argon and BaO is rather weak leading to the structured solvated spectrum. BaO has a stronger interaction with methane and forms a complex with at least one CH_4 molecule.¹⁰ Finally, the interaction between BaO and nitrogen is sufficiently strong to relax completely the electronic excitation of solvated BaO and to quench its fluorescence.

On the contrary, the BaO product interacts even more weakly with neon than with argon, as shown by the $\text{Ba} + \text{N}_2\text{O}$ chemiluminescence spectrum on neon cluster (Fig. 2 panel d). It presents narrow regularly spaced bands in the range $11\,500\text{--}18\,000\text{ cm}^{-1}$. They suggest vibrational progressions of solvated BaO molecules. Their intensity is very weak compared to the underlying broad emission due to free ejected BaO molecules. However in this case, this is not due to an efficient quenching of the solvated BaO emission by neon as for nitrogen, but to a large increase of the BaO ejection yield in the competition between ejection and solvation of the product. This reveals a decrease of the interaction between BaO and the neon solvent.

This section examined the influence of the solvent nature on the nascent distribution of the electronically excited BaO product in the $\text{Ba} + \text{N}_2\text{O}$ reaction with the late N_2O pick-up. The interaction between the solvated product and the solvent increases along the sequence neon, argon, methane and nitrogen. For neon, argon and methane, this evolution can be directly connected to the increase of the solvent polarisability which is respectively 0.397 , 1.66 and 2.605 \AA^3 .¹⁹ The case of nitrogen is different. Its polarisability, 1.764 \AA^3 , is intermediate between those of argon and methane. The large quenching of the solvated BaO emission can be explained by the formation of a charge transfer intermediate resulting from the 2 eV resonance in e^- per N_2 scattering.²

4.2 Reaction between Ba and N_2O on van der Waals clusters with an early N_2O pick-up: comparison with the late N_2O pick-up results

This section discusses results of the $\text{Ba} + \text{N}_2\text{O}$ reaction performed on van der Waals clusters with an early N_2O pick-up and compares them to the results of late N_2O pick-up presented above. As already said, the early pick-up conditions result in the observation of a reaction product that is a few tens of microseconds old. From bottom to top of the right column of Fig. 2 chemiluminescence spectra on neon, argon and methane clusters are shown. Experiments were not per-

formed on nitrogen clusters because of the absence of solvated BaO emission.

A first feature of the spectra obtained in the early pick-up configuration is the relative decrease of the free BaO emission compared to the solvated BaO one. This is particularly striking in the case of methane (panel e) and argon (panel f) clusters. Indeed, in the early pick-up configuration, the ejection of the BaO product occurs in the reaction region located in the barium cell, *i.e.* far away from the observation zone. In contrast, clusters carry solvated products into the observation region. The residual emission of free BaO molecules results from clusters carrying N_2O molecules that can trap barium atoms effusing from the cell in the observation region. In our opinion, the relative importance of this residual contribution on neon clusters is due to the predominance of the ejection channel upon the solvation one with this solvent.

Another interesting feature concerns the structured spectral contribution on neon clusters (panel g) in the range $12\,000$ to $18\,500\text{ cm}^{-1}$. Strikingly, it is dramatically different from the solvated BaO emission in the late pick-up spectrum (panel d). It exhibits two vibrational progressions which have the same envelope, and are composed of narrow and broad bands, respectively.

4.3 Details of the BaO solvated bands

In order to analyse in more detail the structured part of these chemiluminescence spectra, we have subtracted the underlying spectral contributions due to free BaO emission, that are plotted as dashed lines on Fig. 2. The resulting structured spectra are presented on Figs. 3, 4 and 5 for neon, argon and methane clusters, respectively. Of course no figure is presented concerning N_2 since no solvated BaO emission was observed for these clusters.

4.3.1 Neon clusters. For neon clusters, the structured chemiluminescence in the late N_2O pick-up case is presented on the bottom panel of Fig. 3. It presents narrow BaO molecular bands and two narrower atomic $\text{Ba}(^1\text{P}_1 \rightarrow ^1\text{S}_0)$ and $\text{Ba}(^3\text{P}_1 \rightarrow ^1\text{S}_0)$ lines. The two most intense series can be assigned to the vibrational progressions from $\text{BaO } A^1\Sigma v' = 0$ and $v' = 1$ respectively, towards the different vibrational levels of the ground state. The corresponding intensities calculated

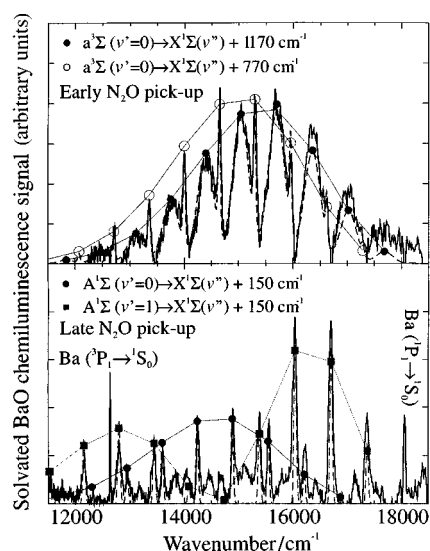


Fig. 3 Solvated BaO chemiluminescence spectra produced by the $\text{Ba} + \text{N}_2\text{O}$ reaction on neon clusters: (a) with an early N_2O pick-up, (b) with a late N_2O pick-up.

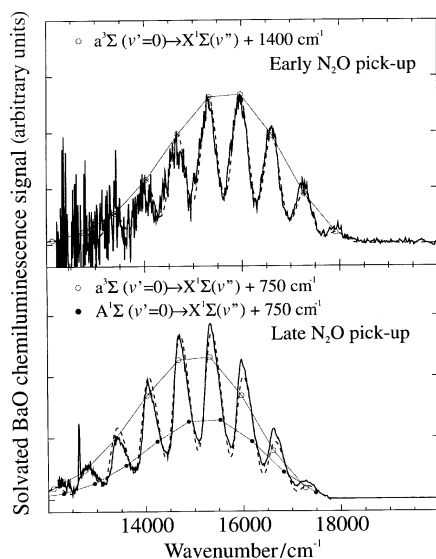


Fig. 4 Solvated BaO chemiluminescence spectra produced by the Ba + N₂O reaction on argon clusters, with a late N₂O pick-up (bottom panel) and an early N₂O pick-up (top panel).

for the free BaO molecule are shown, as filled squares and filled circles for the $v' = 1$ and $v' = 0$ sequences but their positions have to be blue shifted by 150 cm^{-1} to take account for the solvation. The experimental data are fitted by the dashed curve calculated by using the above intensity distribution and a gaussian broadening with a full width at half maximum (FWHM) equal to 50 cm^{-1} . The agreement is good despite a small discrepancy in the blue part of the spectrum where the band intensities are underestimated by the fit. The shift and the broadening of the transitions are the fingerprint of the solvation of emitting BaO molecules on neon clusters. Weak progressions are also visible on the spectrum; they have not been fitted on the figure for reasons of clarity, but they can be assigned to the emission of BaO in the $a^3\Sigma (v' = 0, 1)$ states, which lies 210 cm^{-1} below the $A^1\Sigma (v' = 0, 1)$ ones. So, the nascent BaO product is mainly in the $A^1\Sigma$ electronic state. It is not completely vibrationally relaxed and is very slightly solvated at the surface of the cluster.

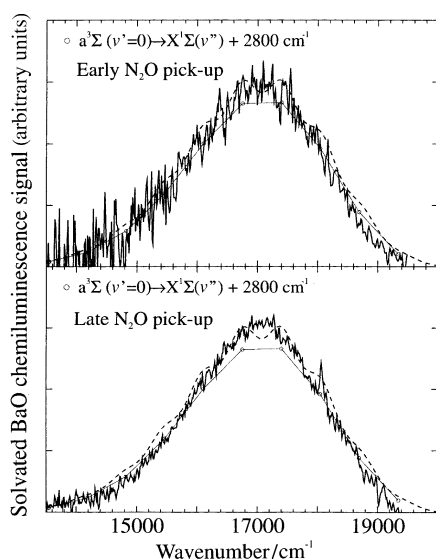


Fig. 5 Solvated BaO chemiluminescence spectra produced by the Ba + N₂O reaction on methane clusters, with a late N₂O pick-up (bottom panel) and an early N₂O pick-up (top panel).

In the early N₂O pick-up case, the situation is quite different: the structured spectrum (Fig. 3 top panel) results from the emission of BaO molecules that have been formed in average $80 \mu\text{s}$ before the detection. The $A^1\Sigma$ state can no longer be populated since its radiative lifetime is about 350 ns ,⁹ and only fluorescence from the $a^3\Sigma$ state is expected. The spectrum presents two vibrational progressions with the same intensity distribution, but, surprisingly with very different band widths. They are both assigned to the emission of BaO in the $a^3\Sigma (v' = 0)$ state. The narrow bands and the broad bands are blue shifted by 770 and 1170 cm^{-1} from the corresponding transitions of the free molecule, respectively. For comparison, the corresponding line intensities calculated for the free BaO molecule are plotted as empty and filled circles, respectively. The experimental data are well fitted by the dashed curve obtained with the above intensity distributions after convolution by gaussian functions with FWHM equal to 50 and 360 cm^{-1} for the narrow and broad bands, respectively. The narrow bands are on the red side of the corresponding broad transitions and, therefore, cannot be assigned to zero phonon lines associated to phonon bands.²⁰ Thus, the two progressions more likely correspond to two different locations of the BaO product: The broad bands to BaO embedded inside the cluster, the narrow ones to BaO less solvated but not really at the cluster surface as nascent BaO. The present 770 cm^{-1} blue shift is indeed much larger than the shift encountered above in the late pick-up case (150 cm^{-1}).

The picture which emerges for the solvated BaO is the following. Immediately after the reaction, electronically excited BaO is both in the $A^1\Sigma$ and a $^3\Sigma$ states, and it is rapidly relaxed enough vibrationally for its emission to originate from $v' = 0, 1$ essentially. After $80 \mu\text{s}$, the $A^1\Sigma$ has decayed to ground state or relaxed to a $^3\Sigma$ by interaction with the cluster, whereas metastable $a^3\Sigma$ has been relaxed vibrationally to $v' = 0$. The BaO molecule, which was solvated slightly, barely in contact with the cluster surface immediately after the reaction, is much more embedded into the cluster $80 \mu\text{s}$ later, with two different locations within the cluster. In contrast with Ba which remains at the surface,^{21,22} the BaO molecule sinks inside the cluster after reaction: this is likely due to its large dipole moment (3D in $A^1\Sigma$ (ref. 23) and probably the same in a $^3\Sigma$) which increases dramatically its interaction with the cluster atoms.

4.3.2 Argon clusters. The structured spectral components of the Ba + N₂O reaction performed on argon clusters are presented in Fig. 4 for the two pick-up configurations.

For the late N₂O pick-up (bottom panel), the spectrum exhibits a set of broad bands. The slight asymmetry of the bands reveals the presence of two vibrational progressions separated by about 200 cm^{-1} .⁷ They can be assigned to the solvated BaO emission from the $A^1\Sigma (v' = 0)$ and a $^3\Sigma (v' = 0)$ states to the different vibrational levels of the ground state. For comparison, the corresponding intensities calculated for the free BaO molecule are plotted (filled and empty circles). However, we have to reduce the ground state vibrational constant ω_e from 669.7 to 653 cm^{-1} and shift their positions to the blue by 750 cm^{-1} . Convolution of this distribution by a gaussian function with $\text{FWHM} = 300 \text{ cm}^{-1}$ gives a spectrum (dashed curve) that fits well the experimental data. The a $^3\Sigma$ contribution to the spectrum is about 1.8 times the $A^1\Sigma$ one.

The structured spectral component obtained in the early N₂O pick-up is presented on the top panel. The bands are now symmetric, indicating the presence of a single progression due to the long lived a $^3\Sigma$ state. The spectrum envelope is very similar to that of the above spectrum and the bands can be assigned to the $a^3\Sigma (v' = 0) \rightarrow X^1\Sigma (v'')$ transitions (empty circles) with a blue shift increased to 1400 cm^{-1} . With a band width increased to 400 cm^{-1} , the calculated spectrum (dashed curve) is in excellent agreement with the experimental data.

As the additional shift (650 cm^{-1}) is nearly exactly equal to the vibrational spacing in the ground state, the question arises whether we missed or not the 0–0 transition in the late pick-up configuration and whether the vibronic transitions are well assigned. Actually, there is no additional visible band in the latter case. Moreover, if we assume its presence, the Franck–Condon factor distribution differs dramatically from the intensity distribution and it becomes quite impossible to fit the experimental data. Thus, we think that our assignment is correct and that the additional shift is due to an enhancement of the BaO solvation between the late and the early pick-up configurations. This is consistent with the larger width of the bands and should correspond to a migration of the product inside the cluster as in the neon cluster case. This is also consistent with the observation that the nascent BaO product is much more solvated on argon clusters than on neon clusters. In particular, (i) BaO is completely vibrationally relaxed on argon clusters, (ii) a major part of the signal comes from the lower $a^3\Sigma$ electronic state, (iii) the bands are six times broader on argon (300 cm^{-1}) than on neon clusters (50 cm^{-1}).

4.3.3 Methane clusters. The solvated BaO spectra obtained in the $\text{Ba} + \text{N}_2\text{O}$ reaction performed on methane clusters are presented in Fig. 5 for the two pick-up configurations. These two spectra do not show any vibrational structure. They have identical shapes and they extend from $14\,000$ to $19\,500\text{ cm}^{-1}$, with a much larger blue shift than on argon clusters. The disappearance of the vibrational structure can be explained by a linewidth larger than the interval between vibrational BaO lines on an argon cluster (653 cm^{-1}). The larger blue shift and the broadening of the transitions indicate that the interaction of BaO is larger with CH_4 than with argon. On argon clusters, a large part of the signal from the nascent BaO is already due to the $a^3\Sigma$ ($v' = 0$) state. The enhancement of the BaO interaction with methane, the similarity between the spectra in the late and early N_2O pick-up configurations, seem to imply that nascent BaO molecules are already relaxed in the $a^3\Sigma$ ($v' = 0$) state and that their solvation does not change substantially in the time interval between them. On bottom and top panels, the line intensities of the free BaO transitions $a^3\Sigma$ ($v' = 0$) \rightarrow $X^1\Sigma$ (v'') are plotted at positions blue shifted by 2825 cm^{-1} with a vibrational interval of 653 cm^{-1} in the ground state (empty circles). The spectrum calculated after convolution of this intensity distribution by a gaussian function with $\text{FWHM} = 675\text{ cm}^{-1}$ (dashed curve) fits correctly the experimental data. However, it still presents some structures which are not visible on the experimental data. Thus, the interaction between BaO and methane seems sufficiently strong to involve a very fast relaxation of BaO in the $a^3\Sigma$ ($v' = 0$) state and a high degree of solvation that will not change in the few tens of microseconds following the chemical reaction, contrary to what happens on neon and argon clusters.

5 Summary and “scenario” of CICR

In this paper, we compared the results of the reaction between Ba and N_2O performed within neon, argon, methane and nitrogen clusters with two different N_2O pick-up configurations. The late N_2O pick-up experiments document the nascent electronically excited product whereas in the early pick-up experiments, the chemiluminescent product is observed a few tens of microseconds after the chemical reaction.

When a chemical reaction occurs on a cluster, there is a competition between the ejection of the product from the cluster surface and its solvation. The reaction path of a direct chemical process like the $\text{Ba} + \text{N}_2\text{O}$ reaction is not greatly

perturbed by the cluster, and the chemiluminescence of the ejected BaO product as measured in the late pick-up experiments, is very similar to that of the gas phase reaction: it is emitted by a hot product that is ejected very rapidly after the reaction and has not enough time to strongly interact with the cluster. In contrast, the cluster has a deep influence on the post reaction processes which affect the solvated product. Firstly, increasing strength of the product/cluster interaction changes dramatically the branching ratio between ejection and solvation by increasing the solvation probability. Secondly, the interaction between the product and the cluster also affects the chemiluminescence of the solvated product.

The late pick-up experiments show that the interaction between BaO and the solvent increases from neon to argon, methane and nitrogen. The BaO–neon interaction is very weak. On neon clusters, the solvated BaO emission originates mainly from the $A^1\Sigma$ $v' = 0$ and $v' = 1$ states. The bands are narrow (50 cm^{-1}) and not much blue shifted (150 cm^{-1}) with respect to the free molecule transitions. On argon clusters, the stronger solvent–BaO interaction results in a complete vibrational relaxation of the product in the $v' = 0$ state, a partial electronic relaxation in the lower $a^3\Sigma$ state, larger broadening (300 cm^{-1}) and blue shift (750 cm^{-1}) of the transitions. The interaction of BaO with methane is even larger leading to a spectrum blue shifted by about 2800 cm^{-1} without any visible structure. This emission is assigned to BaO in the $a^3\Sigma$ ($v' = 0$) state, with a broadening of the lines of about 675 cm^{-1} . Finally, on nitrogen clusters, only the free ejected product emits light. The solvated BaO fluorescence is completely quenched indicating a very strong interaction of the product with nitrogen.

The solvated BaO spectrum changes between the late and the early pick-up experiments, showing a relaxation of the product and a change of its solvation within the cluster. Interestingly, this change is all the more important when the interaction between BaO and the solvent is weak. The strong interaction between BaO and methane results in the identity between the two spectra. The nascent BaO product is already relaxed in the $a^3\Sigma$ ($v' = 0$) state and its solvation within the cluster does not change during a few tens of microseconds following the reaction. On argon clusters, the two spectra are different. The nascent product is already vibrationally relaxed in the $a^3\Sigma$ and $A^1\Sigma$ ($v' = 0$) states. In the early pick-up experiment, the emission comes from the $a^3\Sigma$ ($v' = 0$) state. The width (400 cm^{-1}) and the blue shift (1400 cm^{-1}) of the bands are larger than in the late pick-up experiment (300 cm^{-1} and 750 cm^{-1} , respectively), indicating an increase of the product solvation within the cluster. On neon clusters, the change of the solvated BaO spectrum is more dramatic. In the early pick-up experiment, it is a narrow (50 cm^{-1}) band spectrum slightly blue shifted (150 cm^{-1}), that is mainly emitted by BaO in the $A^1\Sigma$ ($v' = 0$) and $v' = 1$ states. After $80\text{ }\mu\text{s}$, only the long lived $a^3\Sigma$ state remains populated and the vibrational relaxation is complete. The spectrum exhibits a narrow (50 cm^{-1}) and a broad (360 cm^{-1}) band progression, respectively, blue shifted by 770 and 1170 cm^{-1} . BaO is more solvated at two different locations: one embedded inside the cluster, the other one in an intermediate site. In our opinion, the change of the solvated emission between the late and early pick-up spectra is the fingerprint of the BaO migration inside the cluster on a time scale of a few tens of microseconds.

References

- 1 R. D. Levine and R. B. Bernstein, in *Molecular Reaction Dynamics and Chemical Reactivity*, Oxford University Press, 1987.
- 2 C. Gée, M. A. Gaveau, J. M. Mestdagh, M. Osborne, O. Sublemontier and J. P. Visticot, *J. Phys. Chem.*, 1996, **100**, 13421.
- 3 J. M. Mestdagh, M. A. Gaveau, C. Gée, O. Sublemontier and J. P. Visticot, *Int. Rev. Phys. Chem.*, 1997, **16**, 215.

- 4 M. A. Gaveau, C. Gée, J. M. Mestdagh and J. P. Visticot, *Comments At. Mol. Phys.*, 1999, **34**, 241.
- 5 T. E. Gough, M. Mengel, P. A. Rowntree and G. Scoles, *J. Chem. Phys.*, 1985, **83**, 4958.
- 6 C. Alcaraz, P. de Pujo, J. Cuvelier and J. M. Mestdagh, *J. Chem. Phys.*, 1988, **89**, 1945.
- 7 A. Lallement, J. M. Mestdagh, P. Meynadier, P. de Pujo, O. Sublemontier, J. P. Visticot, J. Berlande, X. Biquard, J. Cuvelier and C. G. Hickman, *J. Chem. Phys.*, 1993, **99**, 8705.
- 8 J. P. Visticot, M. A. Gaveau, P. Eulry, M. Lengaigne, J. M. Mestdagh and C. Gée, *Faraday Discuss.*, 1997, **108**, 401.
- 9 S. E. Johnson, *J. Chem. Phys.*, 1972, **56**, 149.
- 10 M. A. Gaveau, B. Schilling, C. Gée, O. Sublemontier, J. P. Visticot, J. M. Mestdagh and J. Berlande, *Chem. Phys. Lett.*, 1995, **246**, 307.
- 11 R. Campargue, *J. Phys. Chem.*, 1984, **88**, 4466.
- 12 C. E. Klots, *Nature (London)*, 1987, **327**, 222.
- 13 J. Farges, M. F. de Feraudy, B. Raoult and G. Torchet, *Surf. Sci.*, 1981, **106**, 95.
- 14 G. Torchet, J. Farges, M.F. de Feraudy and B. Raoult, *Ann. Phys. Fr.*, 1989, **14**, 245.
- 15 J. Cuvelier, P. Meynadier, P. de Pujo, O. Sublemontier, J. P. Visticot, J. Berlande, A. Lallement and J. M. Mestdagh, *Z. Phys. D: At., Mol. Clusters*, 1991, **21**, 265.
- 16 A. J. Bell, J. M. Mestdagh, J. Berlande, X. Biquard, J. Cuvelier, A. Lallement, P. Meynadier, O. Sublemontier and J. P. Visticot, *J. Phys. D: Appl. Phys.*, 1993, **26**, 994.
- 17 S. R. Long, Y. P. Lee, O. D. Krogh and G. C. Pimentel, *J. Chem. Phys.*, 1982, **77**, 226.
- 18 R. A. Gottscho, J. B. Koffend and R. W. Field, *J. Mol. Phys.*, 1980, **82**, 310.
- 19 U. Hohm and K. Kerl, *Mol. Phys.*, 1990, **69**, 803.
- 20 K. K. Rebane, *Impurity Spectra of Solids: Elementary Theory of Vibrational Structure*, Plenum Press, New York—London, 1970.
- 21 J. P. Visticot, P. de Pujo, J. M. Mestdagh, A. Lallement, J. Berlande, O. Sublemontier, P. Meynadier and J. Cuvelier, *J. Chem. Phys.*, 1994, **100**, 158.
- 22 M. Briant, M. A. Gaveau, J. M. Mestdagh and J. P. Visticot, *J. Chem. Phys.*, 2000, **112**, 1744.
- 23 H. S. Schweda, A. Renn, A. Büsener and H. Hese, *Chem. Phys.*, 1985, **98**, 157.

Paper a908930f